PHOTOMETRIC-CORRECTED ALBEDO MAPS OF TETHYS BY CASSINI-VIMS. G. Filacchione[1], M. Ciarniello[1], E. D'Aversa[1], F. Capaccioni[1], P. Cerroni[1], B. Buratti[2], R. N. Clark[3], K. Stephan[4], C. Plainaki[5], [1]INAF-IAPS, Rome, Italy (corresponding author: gianrico.filacchione@iaps.inaf.it), [2]Jet Propulsion Laboratory, California Institute of Technology, Pasadena, CA, USA, [3]PSI Planetary Science Institute, Tucson, AZ, USA, [4]DLR, German Aerospace Center, Berlin, Germany, [5]ASI, Italian Space Agency, Rome, Italy.

Introduction: We report about the derivation of visible and infrared albedo maps and spectral indicators of Tethys from Cassini-VIMS data. The application of a photometric correction to icy surfaces hyperspectral data is a necessary step to remove illumination and viewing effects from the I/F spectra, to compute spectral albedo and to correctly associate spectral variations to changes in composition or physical properties of the surface. In this work we are adopting the photometric correction proposed by [1] to derive albedo maps of Saturn's icy moons from disk-resolved Cassini VIMS-VIS data. After having applied this method to Dione's data [2] we present the results achieved for Tethys.

Tethys dataset returned by Cassini-VIMS: During the entire Cassini mission (2004-2107) VIMS has acquired Tethys surface on more than 280,000 pixels. Among those we have selected about 110,000 pixels that simultaneously fulfill the following conditions: 1) they have an unsaturated signal < 4,000 DN; 2) they have an incidence angle $i \leq 80°$, an emission angle $e \leq 80°$ and a phase angle $10° \leq g \leq 90°$; 3) they are acquired from a distance≤100,000 km, corresponding to spatial resolutions of 50 and 17 km/px in VIMS-Vis nominal and high resolution modes, respectively. This choice allows us to remove pixels taken at very oblique views and in the opposition effect regime which cannot be corrected by the photometric model we are using. VIMS data are calibrated according to RC17 pipeline [3].

Photometric Correction: the details of the method are fully described in [2] and are not repeated here. In summary, the radiance factor $I/F(\lambda,i,e,g)$ measured by VIMS in a given geometry (i,e,g) is given by

$$\frac{I}{F}(\lambda,i,e,g) = D(i,e,g)F(\lambda,g) \qquad 1.)$$

where $D(i,e,g)$ is the disk function and $F(\lambda,g)$ is the phase function which includes the albedo. The disk function follows the definition given by [1]. The phase function is computed by means of a 2nd degree polynomial fit applied to all Tethys data, without any distinction between dark and bright or leading and trailing hemiphere areas. It is therefore an average value for the entire surface:

$$F(\lambda,g) = a + bg + cg^2 \qquad 2.)$$

The best-fit coefficients (a,b,c) are reported in Table 1 for the R=700 nm, G=550 nm, B=440 nm wavelengths. The method allows to compute the equigonal albedo $a(\lambda,g)$ as extrapolated at g=0° from the polynomial fit. We note that this calculation do not account for the opposition sourge: for this reason, the equigonal albedo turns out to be lower lower than the normal albedo $A(\lambda,g)$ for g=0° and i=e as defined by [4].

Coefficient	B=440 nm	G=550 nm	R=700 nm
a	0.7711	0.8136	0.7684
b	-0.0049	-0.0050	-0.0041
c	1.503E-6	-8.763E-7	-6.426E-6

Table 1. Tethys average phase function coefficients derived for RGB wavelengths.

Albedo map rendering: The method used to build the albedo map is the same as described in [5,6]. Each individual VIMS pixel fulfilling the previously reported geometry conditions has been photometrically corrected by means of phase function $F(\lambda,g)$ with the coefficients reported in Table 1 and by the disk function $D(i,e,g)$ and then projected on a cilindrical grid map rendered with a spatial sampling of 0.5°x0.5°/bin along longitude and latitude axes corresponding to a spatial resolution of 4.7 km/bin at the equator. This procedure is followed independently for each RGB channel. Notherworthly, the selected *(i,e,g)* angles ranges are very broad: for comparison, ISS albedo map of Tethys [7] was built with data taken on a very limited phase range (from 10° to 30°). For the VIMS dataset we have relaxed the filtering range to achieve a more extended spatial coverage. As a consequence of this choice, the photometric correction is less accurate for high illumination and viewing angles resulting in some photometric residuals, described ahead. In case of redundancy above a given 0.5°x0.5° bin, the average value is shown on the albedo map in Fig.1. The albedo map covers all longitudes, with the exception of a gap in the middle of the trailing hemisphere, and almost all latitudes between ±80°. Apart the largest impact craters indicated on the map, the dark equatorial lens [7,8] located across the leading hemisphere and

caused by the bombardment of high energy (>10 keV) electrons trapped in the saturnian magnetosphere is clearly visible. The lens encompasses the meridional rim of the large Odyseeus crater and appears to be not completely symmetric with respect to the equator but it is more extended towards northern latitudes (22°) than on southern (-15°) at lon=90° meridian. The asymmetric spatial distribution of the lens could be the consequence of the disturbances occuring in the planetary magnetic field which is not well-aligned starting from the orbit of Tethys and this affects how the electrons travel past the moon [9].

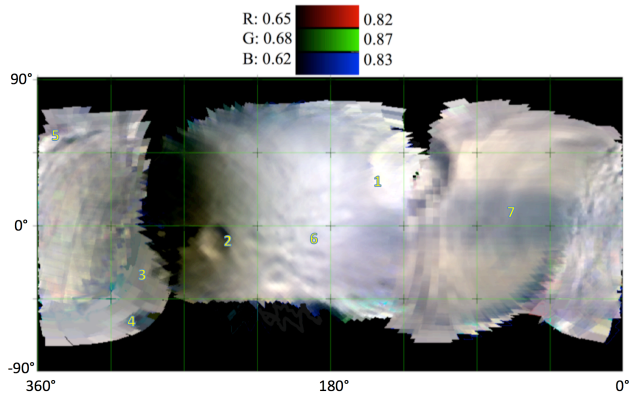

Figure 1. *VIS color albedo map of Tethys rendered at R=700 nm, G=550 nm and B=440 nm colors. Labels indicate impact craters: 1) Odysseus, 2) Penelope, 3) Ajax, 4) Antinous, 5) Telemachus, 6) Dolius. The "Equatorial Lens" generated by the impact of high energy magnetosperic electrons on the leading hemisphere equatorial region is indicated by label 7).*

A dark color arc-shaped area starting from lon=45° at the equator and extending up to lon=90°, lat=-45° is a photometry correction residual. The broad darkening departing from the middle of the trailing hemisphere (lon=270°), including Penelope and Ajax craters is visible on the map. Several different interpretations have been offered to explain this darkening: it could be the result of the alteration caused by bombardment of thermal-suprathermal plasma and by deposition of altered dark particles [7]. Another possibility is given by the combination of Rayleight scattering caused by submicron particles (both water ice and contaminants) and an UV absorber [3]. Finally, according to [10], the UV-VIS darkening observed on the traling hemisphere is caused by the deposition of E ring grains in which the organic material (up to 25% as measured in Enceladus plumes) undergoes to radiolytic alteration causing a darkening/reddening of the particles.

The photometric correction and mapping method here exposed is currently under exploitation to derive similar albedo maps at multiple visible and infrared wavelengths useful to trace the distribution of several spectral indicators, e.g., slopes, water ice band parameters [11] and to correlate them with morphological features of the surface. We underline that such a result has an inter-disciplinary impact since a more detailed knowledge of the surface's spectral properties can provide constraints on the evolution and alteration history of Tethys in the context of the entire saturnian system.

References: [1] Shkuratov Y. et al. (2011) *Planet. Space Sci.* 59, 2011). [2] Filacchione G. et al. (submitted) *GRL*. [3] Clark, R. N. et al. (2012), *Icarus*, 218, 831-860. [4] Hapke, B. (1993) Theory of Reflectance and Emittance Spectroscopy, Cambridge. [5] Filacchione G. et al. (2016) *Icarus,* 274, 334-349. [6] Filacchione G. et al. (2016) *Icarus,* 271, 292-313. [7] Schenk, P et al. (2011) *Icarus*, 211, 740-757. [8] Paranicas, C. (2014), *Icarus*, 234, 155-161. [9] Paranicas, C. (2018), *Icarus*, 302, 560-564. [10] Hendrix, A. R. (2018), *Icarus*, 300, 103-114. [11] Filacchione, G. (2012), 1064-1096.